






Ecdysone exerts biphasic control of regenerative signaling, coordinating the completion of regeneration with developmental progression

Faith Karanja^a, Subhshri Sahu^a , Sara Weintraub^a, Rajan Bhandari^a, Rebecca Jaszczak^a , Jason Sitt^a, and Adrian Halme^{a,1} 

^aDepartment of Cell Biology, University of Virginia School of Medicine, Charlottesville, VA 22902

Edited by Lynn Riddiford, Friday Harbor Laboratories, University of Washington, Friday Harbor, WA; received August 19, 2021; accepted November 13, 2021

In *Drosophila melanogaster*, loss of regenerative capacity in wing imaginal discs coincides with an increase in systemic levels of the steroid hormone ecdysone, a key coordinator of their developmental progression. Regenerating discs release the relaxin hormone Dilp8 (*Drosophila* insulin-like peptide 8) to limit ecdysone synthesis and extend the regenerative period. Here, we describe how regenerating tissues produce a biphasic response to ecdysone levels: lower concentrations of ecdysone promote local and systemic regenerative signaling, whereas higher concentrations suppress regeneration through the expression of *broad* splice isoforms. Ecdysone also promotes the expression of *wingless* during both regeneration and normal development through a distinct regulatory pathway. This dual role for ecdysone explains how regeneration can still be completed successfully in *dilp8* mutant larvae: higher ecdysone levels increase the regenerative activity of tissues, allowing regeneration to reach completion in a shorter time. From these observations, we propose that ecdysone hormone signaling functions to coordinate regeneration with developmental progression.

ecdysone | regeneration | Broad | *wingless* | Dilp8

As tissues develop, their capacity to regenerate is often diminished (1, 2). Often, loss of regenerative capacity is developmentally regulated and coincides with changes in systemic hormone signaling. For example, loss of regenerative capacity in the heart tissues of *Xenopus laevis* and mice is preceded by a sharp increase in systemic thyroid hormone levels (3, 4). Similarly, *Drosophila melanogaster* imaginal discs (larval precursors to adult tissues) lose regenerative ability near the end of larval development (5), coinciding with an increase in systemic levels of the steroid hormone ecdysone, a key coordinator of *Drosophila* developmental progression (6, 7). Regulating systemic levels of ecdysone is a crucial part of the *Drosophila* regenerative response. Regenerating imaginal discs synthesize and release the relaxin hormone *Drosophila* insulin-like peptide 8 (Dilp8), which signals to the brain and endocrine organs through the Lgr3 relaxin receptor to limit ecdysone synthesis (8–13). Reduced ecdysone biosynthesis extends the larval developmental period, providing damaged imaginal discs additional time to regenerate (5, 14).

Although the increased synthesis of thyroid hormone in vertebrates and ecdysone in *Drosophila* constrains regenerative capacity, both hormones are still present at low levels during the regeneration-competent periods of development (3, 4, 7, 15). This basal hormone signaling is likely to be necessary for regeneration to occur. In moths (16), *Sarcophaga* (17), and fiddler crab (18, 19), loss of ecdysteroid signaling restricts regenerative capacity in these organisms. In vitro experiments with *Sarcophaga* leg imaginal discs demonstrate that the absence of ecdysone in culture limits the expression Wingless (Wg), a critical regenerative signal, at the wound site (17).

To better understand how hormones regulate regeneration, we examined how manipulating ecdysone signaling affects both

systemic and local regenerative pathways in the *Drosophila* wing imaginal disk. It has been shown that near the end of larval development, ecdysone signaling in imaginal discs triggers the down-regulation of Chinmo, a BTB-POZ transcription factor that promotes the regenerative activity of imaginal tissues. Ecdysone also promotes the up-regulation of a splice isoform, the BTB-POZ transcription factor Broad, which suppresses Chinmo and regeneration (20). We build on this finding and show here that ecdysone signaling suppresses regeneration at the end of larval development through the expression of multiple splice isoforms of Broad, some also expressed during regeneration in damaged discs, which can each limit the regenerative expression of Wg and also act to determine the duration of the regenerative response. Here we also demonstrate that whereas ecdysone signaling is limited during regeneration by Dilp8 expression, it remains necessary for the regenerative response. We show that ecdysone signaling is cell-autonomously essential for regenerative activity and Wg expression in the disk. Experimentally increasing ecdysone levels up to a certain threshold promotes Wg expression in regenerating discs through a Broad-independent pathway. This dual role for ecdysone in promoting and limiting regeneration helps explain how *dilp8*[−] mutant larvae, which lack the regenerative checkpoint delay

Significance

For most organisms, regenerative capacity varies at different stages of development. Changes in regenerative capacity often correlate with significant changes in systemic hormone signaling. Previous studies have independently demonstrated the positive and negative effects of systemic hormone signals on the regenerative activity of tissues. Here, we report that regenerating *Drosophila melanogaster* tissues produce a biphasic response to ecdysone steroid hormone levels. Below a certain threshold, ecdysone promotes regenerative activity in damaged imaginal discs. As development progresses, ecdysone levels increase above this threshold and suppress regeneration via the sequential expression of Broad transcription factor splice isoforms. Our findings describe how systemic hormone signals can direct regenerative activity to coordinate regeneration completion with developmental transitions.

Author contributions: F.K., S.S., S.W., and A.H. designed research; F.K., S.W., R.B., R.J., and J.S. performed research; F.K. and J.S. analyzed data; and F.K., S.S., and A.H. wrote the paper.

The authors declare no competing interest.

This article is a PNAS Direct Submission.

This article is distributed under Creative Commons Attribution-NonCommercial-NoDerivatives License 4.0 (CC BY-NC-ND).

¹To whom correspondence may be addressed. Email: ajh6a@virginia.edu.

This article contains supporting information online at <http://www.pnas.org/lookup/suppl/doi:10.1073/pnas.2115017119/-DCSupplemental>.

Published January 27, 2022.

following damage, can still regenerate their wing discs during the shorter regenerative period. Therefore, ecdysone's biphasic regulation of regenerative activity gives *Drosophila* larvae the ability to coordinate the completion of regeneration with the end of the larval period.

Results

Ecdysone Limits Regenerative Repair of Wing Imaginal Discs. In order to determine how ecdysone signaling regulates regenerative activity, we assessed how developmental timing and changes in ecdysone titer regulate regenerative outcomes following X-irradiation damage to wing imaginal discs. *Drosophila* larvae exposed to X-irradiation during early third larval instar (L3; 80 h after egg deposition [AED] at 25 °C) can regenerate their wing tissues almost entirely, with only a few adult wings from irradiated larvae exhibiting minor defects (Fig. 1 A and B and *SI Appendix, Fig. S1A*). The regenerated adult wings also match the size of undamaged control wings (Fig. 1C). In contrast, larvae irradiated later, almost prepupal stage (late L3, 104 h AED at 25 °C), produced adult wings with a greater frequency of malformations in wing veins and margin (Fig. 1 A and B) and failed to match the undamaged wing size (Fig. 1C). These differences in regenerative capacity correlate with the ability to activate the regenerative checkpoint. Irradiation at 80 h AED produces a robust checkpoint activation and developmental delay, whereas irradiation at 104 h AED fails to activate the regeneration checkpoint and delay (Fig. 1D). These results are consistent with previous observations that identified this regeneration restriction point (RRP), a developmental time point when damage no longer activates the regenerative response (5, 21). This transition through the RRP impacts regenerative signaling in damaged wing discs, as seen in damage-induced expression of *dilp8*. Dilp8 is a critical regulator of the systemic response to regeneration and a valuable marker for regenerative activity in damaged tissues. Consistent with the reduced regenerative activity, we observe reduced activation of *dilp8* expression (Dilp8::GFP) in wing discs damaged at progressively later times in larval development (Fig. 1E and *SI Appendix, Fig. S1B and C*).

To further demonstrate changes in regenerative signaling with development in this study, we measured irradiation-induced Wg expression. Wg, a critical regenerative morphogen, is up-regulated in the regeneration blastema following targeted damage (21). In irradiation damaged tissues, Wg expression in the hinge region surrounding the wing pouch defines the radiation-resistant cells that contribute to regeneration (22). Upon quantifying Wg expression in the dorsal hinge of irradiated larvae, we found that irradiation pre-RRP (80 h AED) produces a significant increase in Wg expression, which is no longer observed as larvae transit the RRP (Fig. 1F and *SI Appendix, Fig. S1D and E*). These results demonstrate that the loss of regenerative response seen as larvae transit the RRP is accompanied by an inability to activate the expression of Wg and Dilp8, key mediators of local and systemic regenerative processes.

As larvae approach the L3/pupa transition, circulating levels of ecdysone increase rapidly and promote the exit from the larval period (15, 23). To determine whether increased ecdysone titer is sufficient to limit regenerative activity in wing discs, we ectopically increased ecdysone levels by feeding larvae food containing 20-hydroxyecdysone (20E), an active form of this steroid hormone. Larvae damaged pre-RRP (80 h AED) and fed food containing 0.3 mg/mL 20E no longer completely regenerate their imaginal discs (*SI Appendix, Fig. S2A and B*) but instead produce malformed (*SI Appendix, Fig. S2C*) and smaller (*SI Appendix, Fig. S2D*) adult wings. Furthermore, feeding low levels of 20E (0.1 mg/mL) to larvae irradiated post-RRP (104 h AED) produces a synergistic increase in adult

wing malformations (*SI Appendix, Fig. S2E–G*) and suppression of regenerative growth (*SI Appendix, Fig. S2H*). Together, these observations support a model that the increasing levels of systemic ecdysone signaling at the end of larval development suppress regenerative signaling and growth in wing imaginal discs.

Ecdysone Signaling in the Wing Disk Is Necessary for Suppression and Activation of Regenerative Signals. Although the 20E feeding experiments above demonstrate that increasing systemic ecdysone limits the regeneration observed in adult wing tissues, it remained unclear whether ecdysone signaling acts directly on regenerating tissues to suppress regenerative activity or indirectly through other tissues. To test the tissue-autonomous requirement for ecdysone signaling in regenerating wing discs, we expressed a dominant-negative allele of the ecdysone receptor (24) in the dorsal compartment of the wing pouch using *Beadex*-driven, Gal4-UAS expression (*Bx > EcR.A^{DN}*) (*SI Appendix, Fig. S3A*). After the RRP, regeneration-induced expression of the Dilp8 is limited (Fig. 1 G and I and *SI Appendix, Fig. S3B*), reflecting the reduced regenerative activity in these tissues. However, we see that targeted inhibition of ecdysone signaling in the dorsal wing pouch significantly increases *dilp8* expression in larvae damaged at 104 h AED (Fig. 1 H and I and *SI Appendix, Fig. S3B*), suggesting that the regenerative Dilp8 expression in these post-RRP tissues is limited by ecdysone signaling.

We also examined the damage-induced expression of Wg at the dorsal hinge region of the wing pouch (*SI Appendix, Fig. S3A*). Inhibition of ecdysone signaling in the dorsal pouch leads to an overall decrease in Wg expression at the hinge in undamaged tissues (Fig. 1G and *SI Appendix, Fig. S3C*), an observation we address more specifically later in this study. We know that post-RRP, damage in the regeneration incompetent discs induces no change in Wg expression at the dorsal hinge (Fig. 1F and *SI Appendix, Fig. S1D and E*). However, in contrast to control discs, limiting ecdysone signaling in the wing discs permits a damage-induced increase in dorsal hinge Wg expression in post-RRP wing discs. This increase in Wg expression is similar to what we see in regeneration competent discs pre-RRP (Fig. 1 H and J and *SI Appendix, Fig. S3C*). These data demonstrate that at the end of larval development, ecdysone signaling acts tissue-autonomously in wing discs to suppress critical local (hinge-Wg up-regulation) and systemic (*dilp8* expression) signaling events associated with regeneration.

Since circulating ecdysone is present at lower levels at earlier stages of larval development when the wing discs can regenerate (15), we wanted to determine whether ecdysone regulates regeneration signaling in *Drosophila* wing discs damaged pre-RRP (80 h AED). To assess this, we X-irradiated control and *Bx > EcR.A^{DN}* larvae when regenerative activity is high (80 h AED). Consistent with the findings in *Sarcophaga* leg disk regeneration in vitro (17), we observed that ecdysone signaling is necessary for the activation of regenerative signaling pathways following early damage. There is a clear inhibition of *dilp8* expression in the regenerating dorsal wing of *Bx > EcR.A^{DN}* larvae compared to controls (Fig. 1 K–M and *SI Appendix, Fig. S3D*). Ecdysone signaling is also necessary for the increased expression of Wg in the dorsal hinge following damage as we observed reduced expression of Wg at the dorsal hinge of tissues expressing *Bx > EcR.A^{DN}* compared to controls (Fig. 1 K, L, and N, and *SI Appendix, Fig. S3E*). We also saw the requirement of ecdysone signaling in the regenerative activity induced by targeted genetic damage via expression of the *Drosophila* TNF- α homolog, *eiger* (*Bx > egr*). *Eiger* overexpression in wing discs produces localized damage and elicits strong Wg and Dilp8 expression in the regeneration blastema (21) (*SI Appendix, Fig. S3F*). We saw that expression of *EcR.A^{DN}* decreases *eiger*-induced Wg and Dilp8 expression in the damage

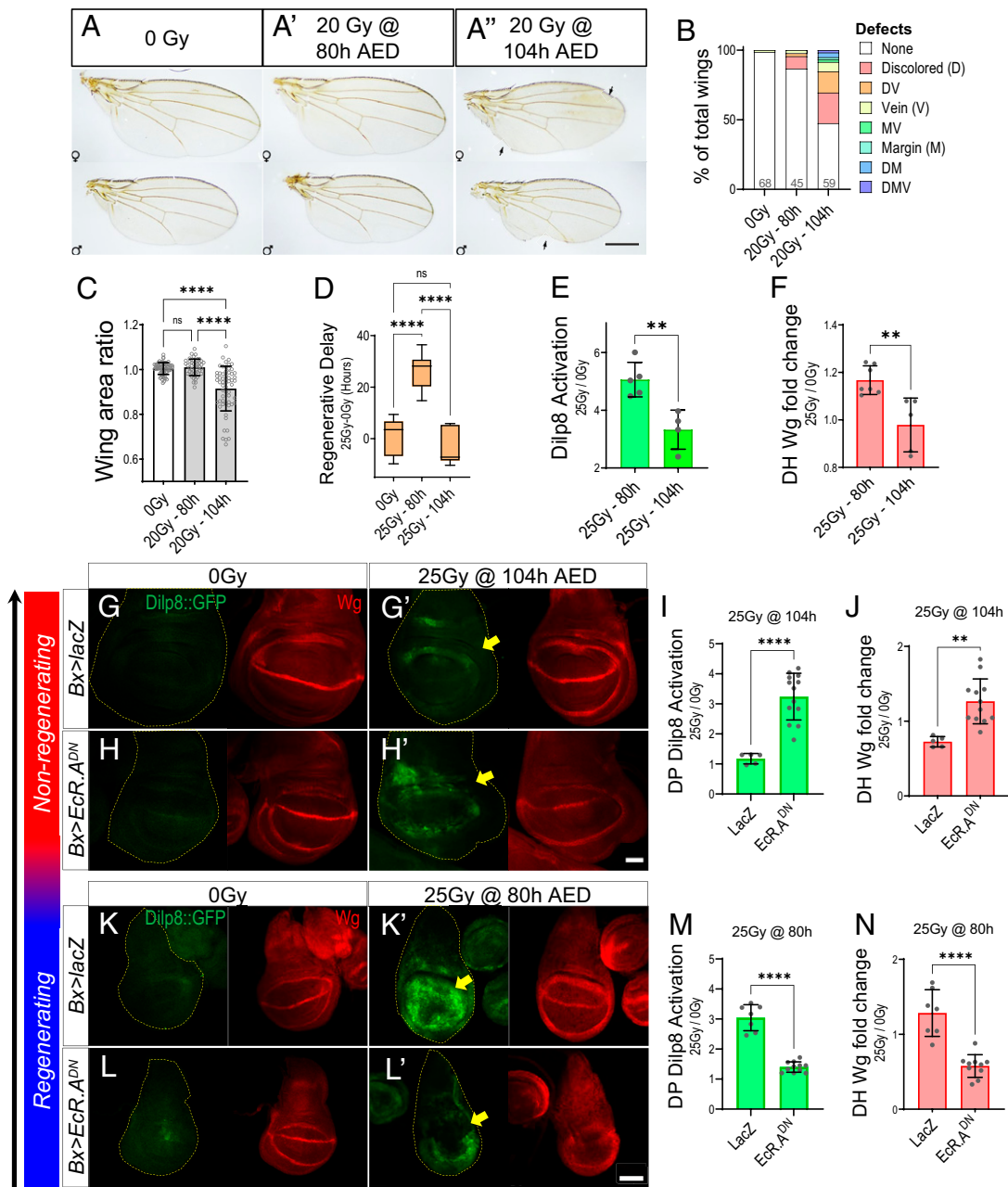


Fig. 1. Ecdysone signaling is necessary for the suppression and activation of regeneration pathways. (A) Representative images of adult female and male wings isolated from undamaged (A); early L3 damaged, 20 Gy X-irradiation at 80 h AED (A'); or late L3 damaged, 20 Gy X-irradiation at 104 h AED larvae (A''). Black arrows indicate defects on late-damaged wings. (Scale bar, 500 μ m.) (B) Adult wings that show individual defects or combinations of defects increase following late damage. The graph shows percentage defective adult wings from larvae that were undamaged (0 Gy), early damaged (20 Gy, 80 h), and late damaged (20 Gy, 104 h) during wing development. Population size is indicated in the graph. (C) Quantification of adult wing size following no damage (0 Gy), early damage (20 Gy, 80 h), and late damage (20 Gy, 104 h). Size of wing measured in the unit area and normalized to undamaged wing size of respective sex. One-way ANOVA with Tukey's test, **** P < 0.0001. (D) Quantification of regenerative delay in undamaged (0 Gy), early damage (20 Gy, 80 h), and late damage (20 Gy, 104 h). One-way ANOVA with Tukey's test, **** P < 0.0001. (E and F) Quantification of relative Dilp8::GFP expression in wing pouch (E) and Wg expression in dorsal hinge (DH) (F) normalized to expression levels in undamaged tissues at each respective time-point tissues. ** P < 0.01, Unpaired t test. (G and H) Representative images of pouch Dilp8::GFP (green) and dorsal hinge Wg (red) expression in 116 h AED wing imaginal discs. The yellow dotted line indicates tissue area. Tissues are expressing lacZ ($Bx > lacZ$) as a control (G and G') or EcR.A^{DN} ($Bx > EcR.A^{DN}$) (H and H') in the dorsal wing pouch region, indicated by yellow arrows. Tissues were undamaged (G and H) or damaged late, 25 Gy at 104 h AED (G' and H'), then isolated 12 h after damage time point. (Scale bar, 50 μ m.) (I and J) Quantification of relative regenerative activity using fold-change in Dilp8::GFP expression in the dorsal wing pouch (DP) (I) and DH Wg expression (J) following late damage (25 Gy, 104 h), in $Bx > lacZ$ and $Bx > EcR.A^{DN}$ wing imaginal discs. Fold-change determined by normalizing to respective undamaged tissues, **** P < 0.0001, ** P < 0.01, Mann-Whitney U test. (K and L) Representative images of pouch Dilp8::GFP (green) and DH Wg (red) expression in 92 h AED wing imaginal discs. The yellow dotted line indicates tissue area. Tissues are expressing lacZ (K and K') or EcR.A^{DN} (L and L') in the dorsal wing pouch region, indicated by yellow arrows. Tissues were either left undamaged (K and L) or damaged early, 25 Gy at 80 h AED (K' and L'), then isolated 12 h after damage time point. (Scale bar, 50 μ m.) (M and N) Quantification of relative regenerative activity using fold-change in Dilp8::GFP expression in the dorsal wing pouch (M) and DH Wg expression (N) following early damage (25 Gy, 80 h), in $Bx > lacZ$ and $Bx > EcR.A^{DN}$ wing imaginal discs. Fold-change determined by normalizing to respective undamaged tissues, **** P < 0.0001, Mann-Whitney U test.

blastema formed in the dorsal compartment of the wing pouch (*SI Appendix, Fig. S3 F–H*).

Together, these findings suggest a dual (activation and suppression) role for ecdysone in the regulation of regenerative activity. During regenerative competence, ecdysone signaling in damaged discs is required to activate Wg and Dilp8 expression, critical signaling events that coordinate the local and systemic regenerative responses, respectively. Following development past the RRP, when imaginal disk regenerative capacity is lost, ecdysone signaling in the disk is required to suppress the activation of these regenerative pathways.

Ecdysone Regulates Regenerative Signaling in a Biphasic, Concentration-Dependent Manner. During the final larval instar, pulses of ecdysone synthesis increase the systemic levels of circulating ecdysteroids in the larvae before a final surge of ecdysone synthesis at the end of larval development activates pupariation pathways and initiate metamorphosis (15). Based on this, we hypothesized that the dual activities of ecdysone signaling that we had observed, necessary for activating regenerative pathways during regenerative competence and suppressing regenerative pathways past the RRP, could reflect the different ecdysone levels at these two points of development. Lower circulating concentrations of ecdysone, such as those found pre-RRP, are necessary for activation of regenerative activity, whereas the higher levels of ecdysone circulating during the prepupal surge interfere with the activation of regeneration pathways. To test this hypothesis, we manipulated circulating 20E levels in larvae by supplementing their food with increasing doses of 20E following X-irradiation damage at 80 h AED. We then measured the regenerative activation of Wg and Dilp8 expression in wing discs 12 h after X-irradiation (Fig. 2A).

We found that feeding larvae ecdysone generally promotes activation of regeneration genes following X-irradiation damage. At all concentrations of 20E feeding, we observed an increase in Dilp8 and Wg expression in damaged wing discs compared with control larvae with no 20E supplement in their food (Fig. 2B–H and *SI Appendix, Fig. S4 A and B*). We also observed that 20E feeding increased the size of the regenerating tissue (Fig. 2I and *SI Appendix, Fig. S4C*). However, the effect of ecdysone feeding was maximized at 0.3 mg/mL 20E concentration. Higher concentrations of ecdysone (0.6 or 1.0 mg/mL) produced a substantial reduction in Dilp8 and Wg expression (Fig. 2B–H and *SI Appendix, Fig. S4 A and B*) and produced no additional increase in growth (Fig. 2I and *SI Appendix, Fig. S4C*). Therefore, 20E feeding produces a biphasic regenerative signaling response in irradiated tissues. However, the biphasic effect of increasing 20E concentrations through feeding was not seen in *eiger*-induced Dilp8 and Wg expression. Both showed a modest but not statistically significant increase in expression with increasing ecdysone levels (*SI Appendix, Fig. S4 D–F*). The differences in ecdysone sensitivity from X-irradiated tissues may reflect the persistence and the intensity of the damage produced in the *Bx > eiger* tissues, which likely maximizes regenerative signaling.

Broad Splice Isoforms Are Necessary to Block Regenerative Signaling after the RRP. To determine how ecdysone limits regenerative signaling, we examined the expression of one of the downstream targets of ecdysone signaling, the BTB-POZ family transcription factors, Broad. Broad is one of the earliest targets of the prepupal ecdysone pulse. Splice isoforms of the transcription factor *broad* (*brZ1*, *Z2*, *Z3*, and *Z4*), named after their respective zinc finger domains (25–27) (*SI Appendix, Fig. S5A*), determine the tissue-specific, temporally regulated signaling events that are initiated in response to ecdysone (28, 29). In addition, BrZ1 has recently been shown to antagonize Chinmo expression in the wing disk, limiting regenerative activity (20).

Using Western blotting of wing disk-derived lysates (Fig. 3A) and immunofluorescence with Broad-targeting antibodies (*SI Appendix, Fig. S5B*), we specifically characterized the spatial and temporal distribution of Broad expression during wing development. Broad splice isoforms are expressed in all wing disk cells throughout L3 development. Based on their distinct molecular sizes (29), we determined that BrZ2 is expressed throughout the L3 stage, but its levels increase as larvae approach pupation. While we could not distinguish BrZ1 and BrZ3 based on size, previous studies have demonstrated a general lack of BrZ3 expression in prepupa imaginal discs (29). In addition, we could verify the emergence of BrZ1 expression in the tissue using Z1-targeted IF (*SI Appendix, Fig. S5B'*). The expression of both BrZ1 and BrZ4 can be detected at 104 h AED and dramatically increases as larvae approach pupariation. Following early damage (80 h AED), the expression of the Broad isoforms is delayed (Fig. 3A). Therefore, the expression of Broad isoforms corresponds to the known changes in ecdysone levels during larval development and regeneration, and increases in Broad expression correlate with loss of regenerative capacity.

To determine whether Broad isoforms participate in the suppression of regenerative capacity at the end of larval development, we examined the effect of isoform-specific or pan-isoform disrupting zygotic *br* mutants (in hemizygous males) (Fig. 3B–H) or pan-isoform targeting *br^{RNAi}* expression (*SI Appendix, Fig. S5E*) on regenerative signaling. Loss of all Broad isoforms in (*br^{ppr-6}npr⁶* or *Bx > br^{RNAi}*) wing discs allows post-RRP discs to express *dilp8* (Fig. 3C and G and *SI Appendix, Fig. S5 C and F–H*). Using the isoform-specific alleles, we determined that BrZ1 and BrZ2 are necessary for restricting *dilp8* expression at the RRP (Fig. 3D and E). Our BrZ3-specific allele *br^{2Bc-2}2Bc²* produced little effect on *dilp8* expression at the RRP, consistent with BrZ3 playing a limited role in wing development (Fig. 3F). We were unable to obtain *BrZ4*-specific mutants to examine *BrZ4* loss-of-function phenotypes.

Examining Wg expression in the wing discs of *br* mutants showed these mutations alter developmental Wg expression. However, we did not see as clear effects on regenerative Wg expression as those seen for regenerative *dilp8* expression. In the *npr⁶* mutant, which disrupts all the broad isoforms, we observed a substantial Wg expression reduction in undamaged tissues' hinge region (Fig. 3C and H). This reduction is similar to what is seen in the Z2-specific allele *br²⁸* (Fig. 3E and H). In contrast, in *br^{ppr-5} (rbp⁵)* mutant discs where the Z1 isoform is specifically disrupted, the hinge expression of Wg is largely normal in undamaged discs, but the expression pattern of Wg in the margin is disrupted (Fig. 3D illustrates a representative example). This phenotype may reflect the role of Broad in regulating Cut expression at the margin (30), but we leave the further examination of this phenotype for later studies. When we examined tissues damaged after the RRP, we saw that none of the isoform-specific mutants produced a substantial increase in Wg expression in discs damaged after the RRE (Fig. 3H).

All *br* mutants used were either nonpupariating or pupal lethal (27, 31). Therefore, we were unable to evaluate whether the increased *dilp8* expression observed in *br* mutants led to improved tissue repair in adult tissues. However, our experiments demonstrate that Broad isoforms mediate the ecdysone-dependent restriction of Dilp8 signaling in post-RRP L3 wing discs.

Broad Isoforms Regulate the Duration of the Regenerative Response in Damaged Discs. Since some Broad isoforms are expressed in regenerating tissues (Fig. 3A), we wanted to determine how the loss of Broad or specific Broad isoforms might affect regenerative activity following early damage (80 h AED) of discs. In early damaged discs, we observed that the pan-isoform mutant

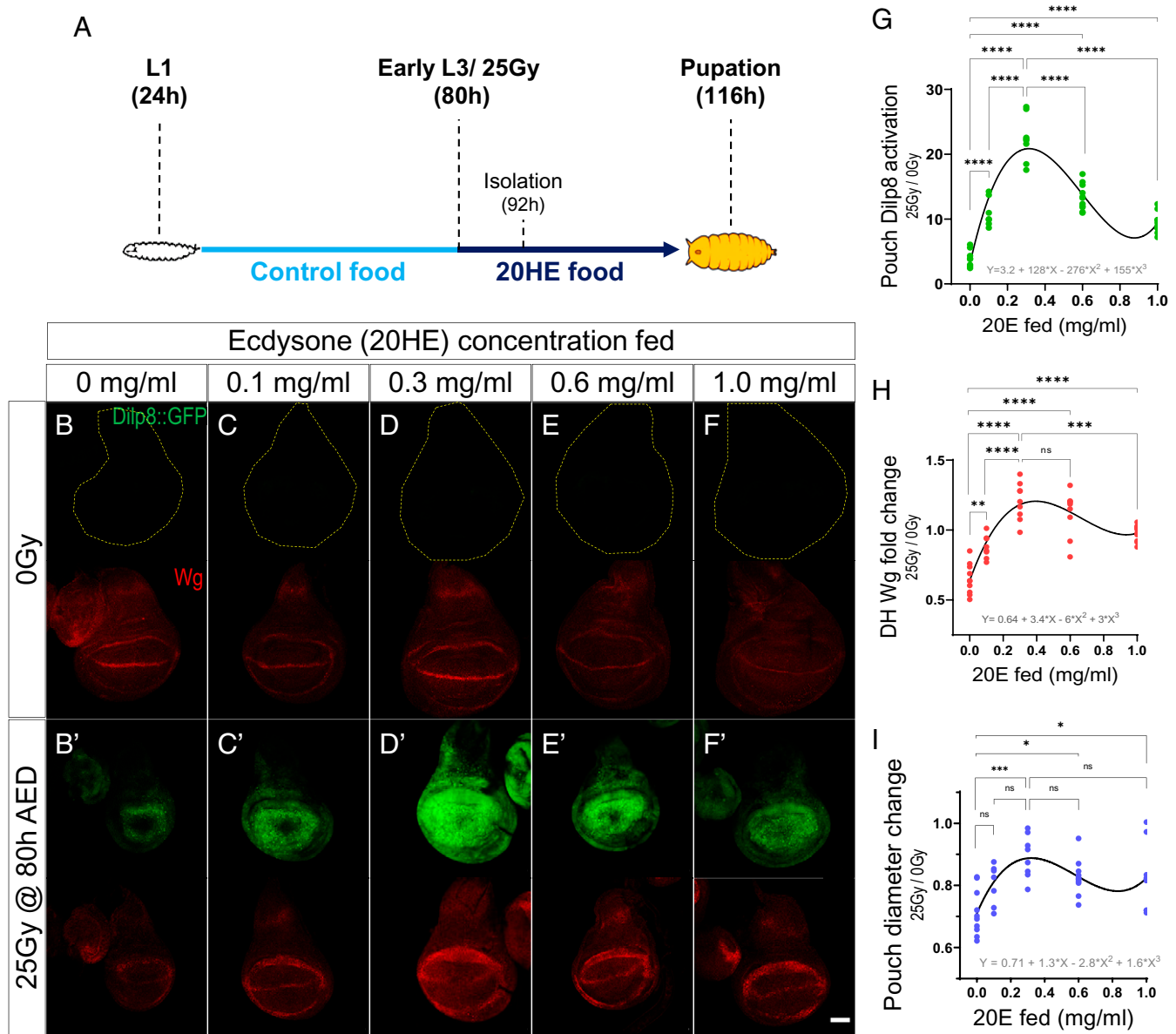


Fig. 2. Ecdysone regulates regenerative signaling in a biphasic, concentration-dependent manner. **(A)** Schematic of ecdysone (20E in ethanol) feeding experiment. *w¹¹¹⁸* larvae were fed various 20E concentrations in early L3 (80 h AED) immediately after irradiation damage (25 Gy at 80 h AED) or no damage (0 Gy). Tissues were isolated 12 h after damage and feeding (92 h AED). **(B–F)** Representative images of pouch Dilp8::GFP (green) and dorsal hinge Wg (red) expression in 92 h AED undamaged (**B–F**) and early damaged (25 Gy at 80 h AED) (**B'–F'**) wing imaginal discs. The yellow dotted line indicates tissue area. *w¹¹¹⁸* larvae were fed 20E: 0 mg/mL (**B** and **B'**), 0.1 mg/mL (**C** and **C'**), 0.3 mg/mL (**D** and **D'**), 0.6 mg/mL (**E** and **E'**), and 1.0 mg/mL (**F** and **F'**). (Scale bar, 50 μ m.) **(G–I)** Quantification of relative regenerative activity using fold-change of Dilp8::GFP expression in the wing pouch (**G**), dorsal hinge (DH) Wg expression (**H**), and pouch diameter (**I**) in 20E fed and early damaged *w¹¹¹⁸* wing imaginal discs. Fold-change determined by normalizing to respective undamaged tissues, Polynomial regression: Dilp8 $R^2 = 0.86$, Wg $R^2 = 0.76$, and Diam. $R^2 = 0.64$. Statistical analysis: one-way ANOVA with Tukey's test, **** $P < 0.0001$, *** $P < 0.001$, ** $P < 0.01$, * $P < 0.05$.

npr⁶ and the Z2 specific mutant *br²⁸* produce higher *dilp8* expression 12-h following damage (*SI Appendix, Fig. S6 A–E*). In addition to differences in the levels of *dilp8* expression, we also observed substantial differences in the duration of *dilp8* expression between the different mutants, with the pan-isoform mutant *npr⁶* and the Z1-specific mutant, *rbp⁵*, producing a more extended *dilp8* expression period compared with control discs, or the Z2-specific mutant *br²⁸* (*SI Appendix, Figs. S6 A–D and S7A*). These results suggest that following early damage when the wing disk can initiate a regenerative response, the amount and duration of *dilp8* expression in the disk is regulated by specific Broad isoforms. We confirmed this result by using *br^{RNAi}* to inhibit all the Broad isoforms and demonstrated that

Bx > br^{RNAi} discs also produce extended *dilp8* expression following damage (*SI Appendix, Fig. S7 E–G*). In contrast to Dilp8 expression, the effects of the Broad isoform mutants on Wg expression during regeneration are less apparent. As described above, the pan-isoform mutant *npr⁶* and the Z2-specific mutant *br²⁸* produce reduced levels of Wg at the hinge region in undamaged tissues (*SI Appendix, Figs. S6 A–D and S7C*). However, all the mutants can produce a similar relative increase in Wg expression following damage (*SI Appendix, Fig. S7D*). Finally, Broad isoforms may also regulate the early events associated with either damage or the initial regenerative response, as we see that the reduction of wing pouch (and overall disk) size following irradiation damage at 80 h AED is much

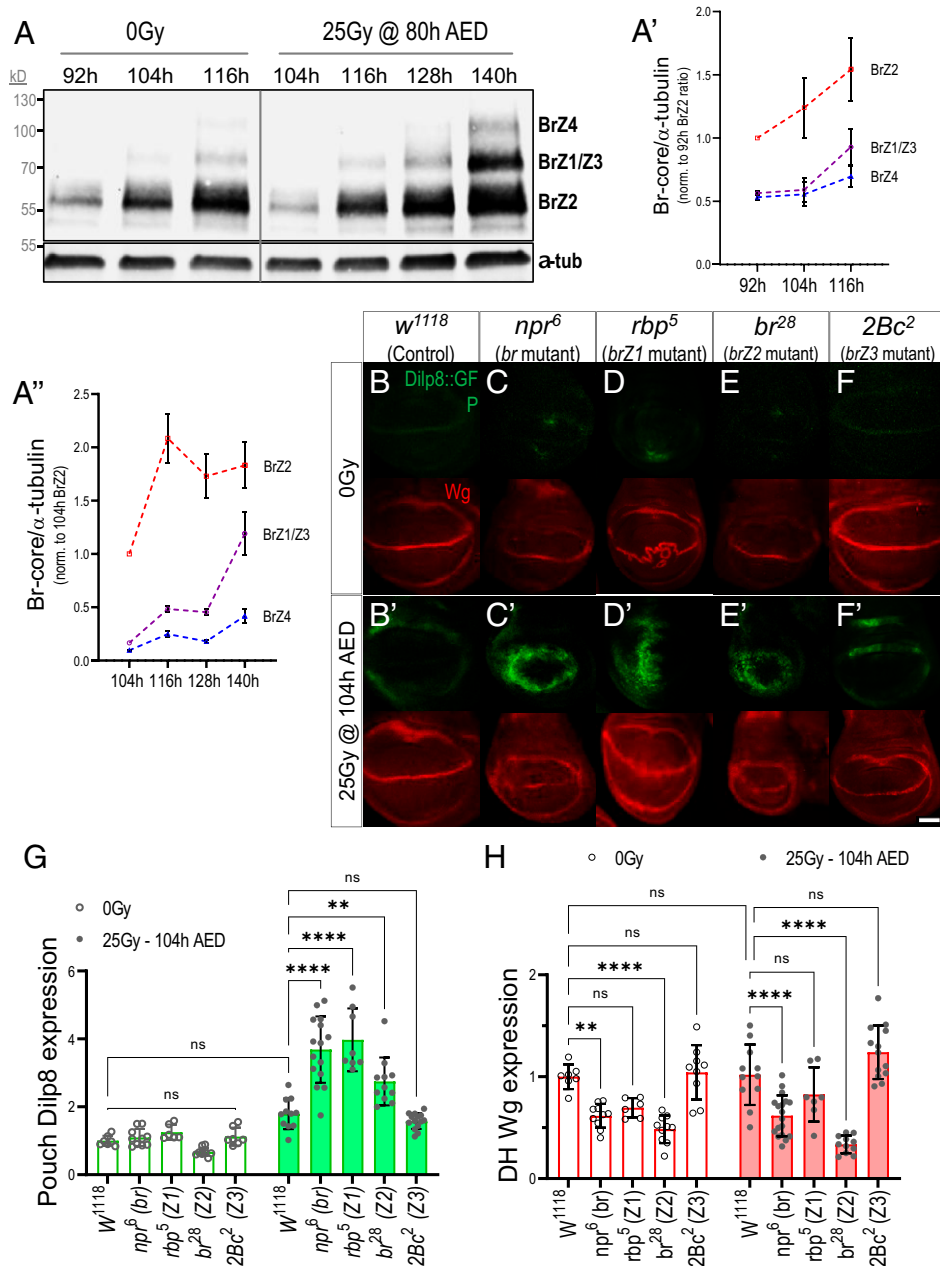


Fig. 3. Broad isoforms are necessary to restrict regenerative activity at the end of larval development. (A) Western blot time course of Broad isoform expression in undamaged and early damaged *w¹¹¹⁸* wing imaginal discs. Tissues were isolated in 12-h intervals. Broad core antibody was used to visualize BrZ4 (~110 kD), BrZ1/3 (~90 kD), and BrZ2 (~55 to 65 kD), while α -tub (~50 kD) as a loading control. Protein size (kDa) ladder, on the left. Quantification of Broad expression in undamaged (A') normalized to 92 h AED BrZ2 expression, $n = 5$. Quantification of Broad expression in damaged (A'') wing discs normalized to 104 h AED BrZ2 expression, $n = 3$. (B–F) Loss of Broad isoforms allows for activation of regenerative activity post-RRP. Images show representative examples of pouch Dilp8::GFP (green) and dorsal hinge Wg (red) expression in 116 h AED wing discs of undamaged (B–F), and late damage (25 Gy at 104 h AED) (B'–F'), control (*w¹¹¹⁸*) (B and B'), and *br* mutants: full *br* mutant (*npr⁶*) (C and C'), *brZ1* mutant (*rbp⁵*) (D and D'), *brZ2* mutant (*br²⁸*) (E and E'), and *brZ3* mutant (*2Bc²*) (F and F'). (G and H) Quantification of regenerative activity in 116 h AED tissues using pouch Dilp8::GFP expression in the (G) and dorsal hinge (DH) Wg expression (H) in *w¹¹¹⁸* and *br* mutants wing imaginal discs. All quantifications normalized to undamaged *w¹¹¹⁸*, ** $P < 0.01$, **** $P < 0.0001$, two-way ANOVA with Tukey's test.

greater in all isoform mutants, especially Z1-specific *rbp⁵* and Z2-specific *br²⁸* mutant discs (SI Appendix, Figs. S6 A–D and G and S7B).

In summary, our loss-of-function analysis demonstrates that the individual Broad isoforms play distinct roles in regulating the regenerative signaling response of wing discs damaged post-RRP. In addition, the Broad isoforms also regulate the extent and duration of Dilp8 signaling produced by discs damaged before the RRP. However, the Broad isoforms show

distinct roles in regulating Wg expression. Based on these observations, we conclude that ecdysone signaling through Broad is necessary to limit both the tissue's competence to produce a regenerative response, as well as the duration of that response.

Expression of Individual Broad Isoforms Is Sufficient to Limit Regeneration. From our loss-of-function experiments, it appears that expression of Broad isoforms may limit the duration of

regenerative response in discs damaged pre-RRP and block the initiation of regenerative activity in discs damaged post-RRP. To examine whether the expression of individual Broad isoforms is sufficient to limit regeneration, we expressed individual Broad isoforms in the wing disk and examined both regenerative signaling and regeneration outcomes in adult wings. When we examined regenerative signaling in 80 h AED-damaged discs, we observe that *Bx-Gal4*-driven expression of BrZ1, BrZ2, and BrZ4 limits both *dilp8* and Wg expression in the dorsal compartment of the wing disk, with BrZ1 and BrZ4 producing the strongest inhibition of regenerative Wg expression (Fig. 4 A–F and *SI Appendix, Fig. S8 A and B*). These distinct effects of Broad isoforms on regenerative Wg and *dilp8* expression were also observed in discs experiencing *eiger*-induced damage. BrZ1, BrZ2, and BrZ4 all reduce *dilp8* expression in these regenerating tissues. Again, BrZ1 and BrZ4 produce the strongest inhibition of Wg expression in the *eiger* damage model (*SI Appendix, Fig. S8 C–I*). Therefore, all three isoforms can limit regenerative signaling in *eiger*-damage discs. Consistent with this, RNAi-inhibition of all the Broad isoforms produces elevated levels of both Wg and *dilp8* in *eiger*-damaged tissues (*SI Appendix, Fig. S8 G–J*).

Constitutive expression of individual Broad isoforms produces substantially deformed adult wings and pupal lethality, making it challenging to assess regenerative outcomes. Therefore, to determine whether expression of the individual Broad isoforms is sufficient to inhibit regeneration, we transiently expressed each of the Broad isoforms in the wing pouch using *m-Gal4* and used *tub-Gal80^{ts}* expression to limit the timing of expression to a 12-h window following irradiation (*SI Appendix, Fig. S9A*). We observed that transient expression of BrZ1, BrZ2, and BrZ4 in undamaged control larvae produces only minor effects on disk patterning and growth (Fig. 4 G and H and *SI Appendix, Fig. S9 B–E*). However, the transient expression of Broad isoforms following early L3 X-irradiation damage profoundly affects wing regeneration. Expression of BrZ1, BrZ2, and BrZ4 results in a high proportion of incompletely regenerated discs and reduced wing blade size. Of the three splice isoforms, BrZ4 produces the most potent inhibition of regeneration, with all the adult wings mispatterned and extremely small (Fig. 4 G and H and *SI Appendix, Fig. S9 B–E*).

In summary, our isoform expression experiments demonstrate that the local expression of individual Broad isoforms in damaged tissues is sufficient to block critical local and systemic regeneration signaling events. Even the transient expression of single Broad isoforms in regenerating tissues can severely attenuate regeneration in these tissues.

Ecdysone Inhibits and Promotes *wg* Expression through Distinct Pathways. We have demonstrated here that ecdysone produces dual effects on regenerative signaling. At lower levels, ecdysone can promote the expression of Wg and *dilp8* in regenerating tissues. At higher levels, ecdysone limits regeneration and the expression of these regenerative signals through the activation of Broad splice isoforms. To better understand how ecdysone produces these distinct effects on regenerative signaling, we examined how ecdysone regulates a regulatory region located ~8 kb downstream of the *wg* coding region (*SI Appendix, Fig. S10A*), which was previously named BRV118 (32) but has more recently been described as *wg* damage responsive enhancer (*wgDRE*) (33). The *wgDRE* is critical for the regenerative activation of *wg* expression following damage. Epigenetic changes at the *wgDRE* toward the end of larval development leads to the loss of regenerative capacity following the RRP (34). However, it is unclear how these epigenetic changes are facilitated.

Using a transgenic reporter of *wgDRE* activity (*wgDRE-GFP*) (34) (*SI Appendix, Fig. S10A*), we observed the attenuation of damage-induced *wgDRE* activity as larvae develop

across the RRP (*SI Appendix, Fig. S10 B and C*). To first determine whether the limitation of regenerative activity by ecdysone at the RRP is mediated through the *wgDRE*, we measured reporter expression in *Bx > EcR.A^{DN}* discs. We saw that blocking ecdysone signaling increases the damage-induced *wgDRE* reporter activity in the dorsal pouch of discs damaged post-RRP (Fig. 5 A, B, and D and *SI Appendix, Fig. S10D*). Therefore, the inhibition of the *wgDRE* in late-damaged tissues is dependent on ecdysone signaling in regenerating disk tissues. Consistent with our earlier observations, the inhibition of the *wgDRE* post-RRP is also dependent on Broad, as late damage can also activate the *wgDRE* in *Bx > br^{RNAi}*-expressing discs (Fig. 5 A, C, and D and *SI Appendix, Fig. S10D*). To determine which Broad isoforms are sufficient to suppress *wgDRE* activity, we examined whether expression of Broad isoforms can suppress the pre-RRP damage-induced activation of *wgDRE*. We saw that expression of BrZ1, BrZ2, and BrZ4 can suppress *wgDRE* activation following early damage (Fig. 5 E–I and *SI Appendix, Fig. S10E*). Based on these results, we conclude ecdysone, via Broad isoform expression, can limit regenerative activity by suppressing the damage-induced activity of the *wgDRE*.

To assess how lower levels of ecdysone function to promote regenerative Wg expression, we first examined how the loss of ecdysone signaling affects Wg expression in undamaged wing discs. We had observed in Fig. 1D that *Bx > EcR.A^{DN}* expression appears to suppress hinge Wg expression in undamaged tissues. To examine this more carefully, we used MARCM to generate GFP-labeled clones that expressed *EcR.A^{DN}*. We observed that *EcR.A^{DN}* expression produced clones that cell-autonomously inhibited Wg expression at the hinge regions of the developing wing disk but not at the margin (Fig. 5 L and M). This inhibition appears to be a transcriptional regulation of *wg* expression, as we saw a similar effect of *EcR.A^{DN}* expression on the activity of a *wg* transcriptional reporter line (*wg-lacZ*) (Fig. 5N). It is possible that ecdysone exerts both its inhibitory and activating effects on Wg expression through the *wgDRE*. However, when we inhibited ecdysone signaling (*Bx > EcR.A^{DN}*) or Broad isoform expression (*Bx > br^{RNAi}*) in early-damaged discs, we saw that neither of these manipulations limited *wgDRE* activation (Fig. 5 E, J, and K and *SI Appendix, Fig. S10E*). Therefore, ecdysone signaling is required for regenerative Wg expression but regulates *wg* transcription independently of Broad and through a regulatory region that is not part of the *wgDRE*. These distinct pathways for ecdysone regulation of Wg are summarized in Fig. 5O.

Ecdysone Signaling Coordinates Regeneration with the Duration of the Larval Period. Damage and regeneration of imaginal discs activates a delay in development that extends the larval development period (regeneration checkpoint). This checkpoint arises from the expression and release of Dilp8 from regenerating tissues (8, 9). Dilp8, through its receptor Lgr3 expressed in both the brain and ecdysone-producing prothoracic gland (PG), limits the ecdysone synthesis (10, 11, 13). This Dilp8-Lgr3 signaling delays the accumulation of ecdysone at the end of the larval period, extending the regenerative competence of imaginal discs and delaying the transition to the pupal phase of development (10, 11). Because Dilp8 activation of the regeneration checkpoint extended the regenerative period of development, we (11, 35, 36) and other researchers (8, 9, 12, 13, 37) have hypothesized that the extra time was required for the repatterning and regrowth required to complete regeneration. However, since we have shown that ecdysone produces a biphasic effect on regenerative signals in the damaged disk, we wanted to test the hypothesis that checkpoint delay was required to accommodate regeneration. To do this, we examined regeneration in homozygous *dilp8⁻* larvae, which produce minimal checkpoint delay following damage (Fig. 6A), therefore having a shorter

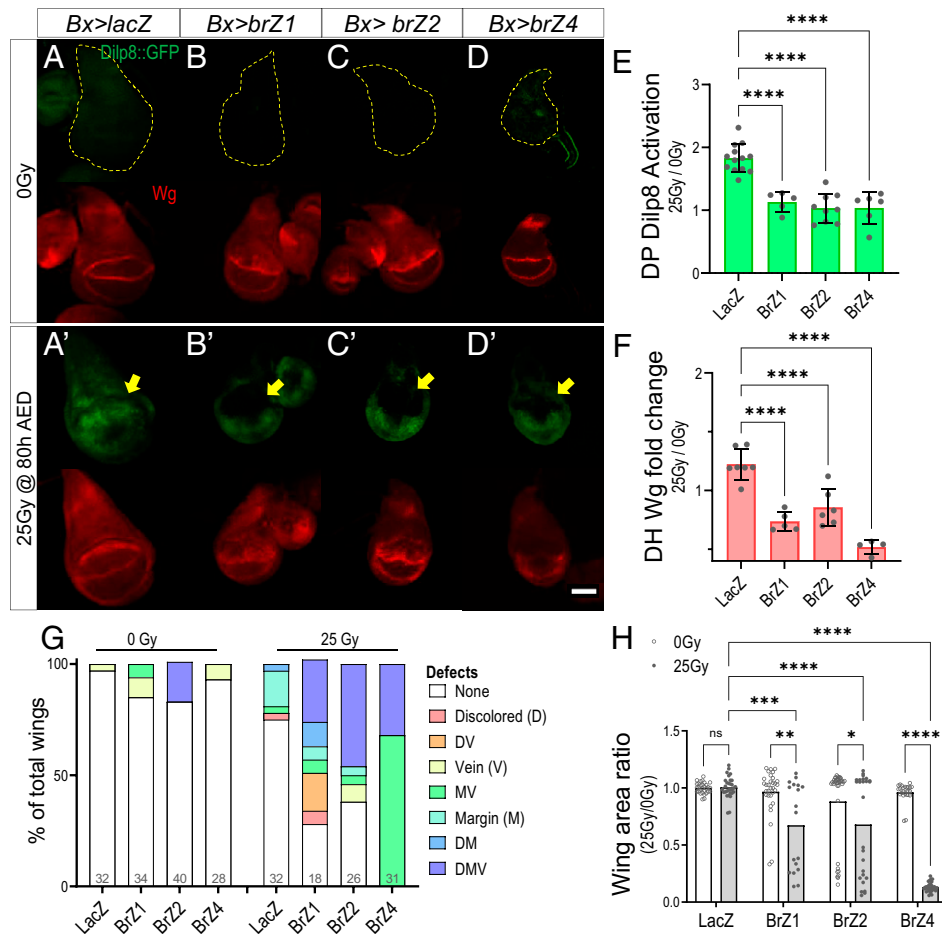


Fig. 4. Broad isoform expression is sufficient to suppress regenerative signaling in damaged imaginal discs. (A–D) Representative images of pouch *Dilp8::GFP* (green) and *Wg* (red) expression in 92 h AED undamaged (A–E) and early damaged 25 Gy at 80 h AED (A'–E') wing imaginal discs. The yellow dotted line indicates tissue area. Tissues are expressing *lacZ* (*Bx > lacZ*) as a control (A and A') or *br* isoforms, *Bx > brZ1* (B and B'), *Bx > brZ2* (C and C'), and *Bx > brZ4* (D and D'). Yellow arrows indicate primary area of analysis. (Scale bar, 50 μ m.) (E and F) Quantification of relative regenerative activity using fold change in dorsal pouch *Dilp8::GFP* expression (E) and dorsal hinge *Wg* expression (F) in early damaged, control *Bx > lacZ* and *br* isoform overexpressing wing imaginal discs. Fold-change determined by normalizing to respective undamaged tissues, **** $P < 0.0001$, one-way ANOVA with Tukey's test. (G) Adult wings that show individual defects or combinations of defects increase following late damage. The graph shows the percentage of defective adult wings from larvae transiently overexpressing *lacZ*, *brZ1*, *brZ2*, and *brZ4* (*rn-gal4*) with no damage (0 Gy) and early damage (25 Gy) during wing development. Population size is indicated in the graph. (H) Quantification of adult wing size for tissue in G. Size of wing measured in unit area and normalized to undamaged *rn > lacZ* wing size of respective sex. Two-way ANOVA with Tukey's test, **** $P < 0.0001$, *** $P < 0.001$, ** $P < 0.01$, * $P < 0.05$.

regenerative period. Unexpectedly, adult flies arising from X-irradiated *dilp8⁻* larvae could regenerate their wing discs as successfully as control *dilp8⁺* (*w¹¹¹⁸*) adults. The lack of regeneration checkpoint delay produced no significant impact on tissue repatterning (Fig. 6B). In fact, we saw that *dilp8⁻* larva produce regenerated adult wings that are closer to the undamaged target size than *dilp8⁺* larvae in which the checkpoint is intact (Fig. 6C and *SI Appendix*, Fig. S11A).

To better understand how *dilp8⁻* larvae can regenerate damaged wing discs despite the attenuated regenerative period, we measured disk growth in undamaged and regenerating discs through the L3 in *dilp8⁺* and *dilp8⁻* larvae. In control larvae, damage retarded disk growth, with regenerating imaginal discs producing a slightly lower growth rate than control larvae (Fig. 6D), with regenerating disk sizes lagging behind undamaged controls between 92 and 116 h AED, when unirradiated larvae pupariate (*SI Appendix*, Fig. S11B). However, during the extended larval period produced by activation of the regenerative checkpoint, the growth of the regenerating wing discs can reach the target size (final size of undamaged discs) by 128 h AED and remains at this size until the end of the larval period

(Fig. 6D and *SI Appendix*, Fig. S11B). In contrast, regenerating tissues in *dilp8⁻* larvae grow substantially faster than undamaged discs (Fig. 6E) (reaching target size by 116 h AED) just before both control and *dilp8⁻* larvae pupate (Fig. 6E and *SI Appendix*, Fig. S11C). When we directly compared the growth of control and *dilp8⁻* imaginal discs, we saw that during normal development, *dilp8⁻* wing discs grow more slowly than control discs (*SI Appendix*, Fig. S11D), whereas regenerating *dilp8⁻* imaginal discs grow much faster than control discs (*SI Appendix*, Fig. S11E).

In summary, we observed that in the absence of the *Dilp8* regeneration checkpoint, ecdysone synthesis is no longer limited, and the regenerative growth of imaginal discs is accelerated such that target disk size is still reached by the end of the shortened larval period. This suggests that the biphasic effect of ecdysone signaling on disk regeneration is capable of coordinating disk regeneration with the duration of the larval period.

While *Dilp8* and checkpoint activation are not necessary for providing additional time to accommodate regenerative growth, checkpoint activity is essential for maintaining the viability of pupae following regeneration. The frequency of pupal lethality

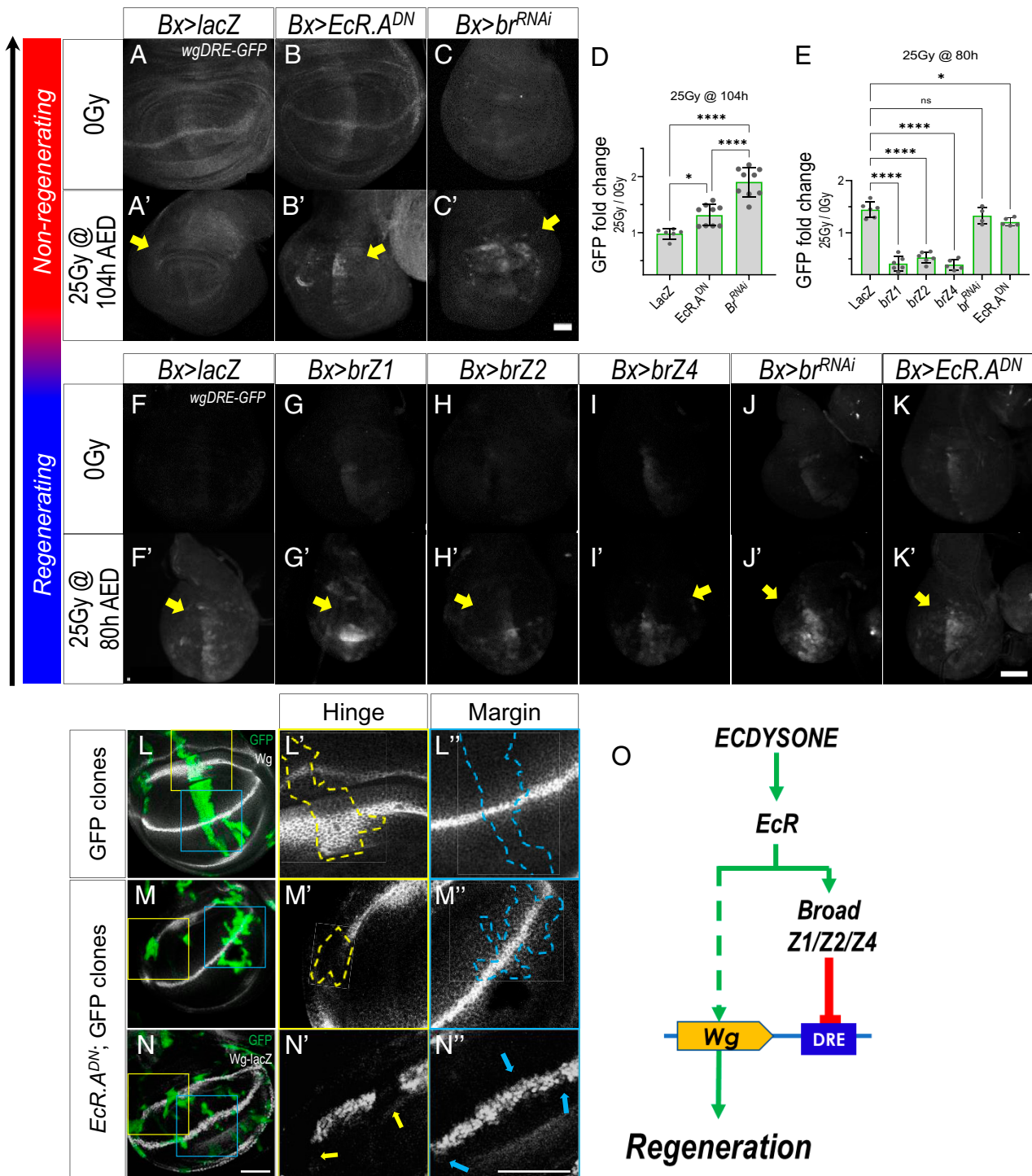


Fig. 5. Ecdysone signaling regulates Wg expression. (A–C) Representative images of wgDRE-GFP (gray) expression in 116 h AED undamaged (A–C) and late damaged (25 Gy at 104 h AED) (A'–C') wing imaginal discs. Yellow arrows indicate the primary area of Gal4-UAS expression. Tissues are expressing lacZ ($Bx > lacZ$) as a control (A and A'), $Bx > EcR^{DN}$ (B and B'), and $Bx > br^{RNAi}$ (C and C'). (Scale bar, 50 μ m.) (D) Quantification of dorsal pouch wgDRE-GFP expression fold-change following late damaged (25 Gy, 104 h), control $Bx > lacZ$, $Bx > EcR^{DN}$, and $Bx > br^{RNAi}$ overexpressing wing imaginal discs. Quantification normalized to respective undamaged tissues. **** $P < 0.0001$, * $P < 0.05$, one-way ANOVA with Tukey's test. (E) Quantification of dorsal pouch wgDRE-GFP expression fold-change following early damaged, control $Bx > lacZ$, br isoform overexpressing, br knockdown, and EcR^{DN} expressing wing imaginal discs. Normalized to respective undamaged tissues, **** $P < 0.0001$, * $P < 0.05$, one-way ANOVA with Tukey's test. (F–K) Representative images of wgDRE-GFP (gray) expression in 92 h AED undamaged (F–K) and early damaged (25 Gy at 80 h AED) (F'–K') wing imaginal discs. Tissues are expressing lacZ ($Bx > lacZ$) as a control (F and F') or br isoforms, $Bx > brZ1$ (G and G'), $Bx > brZ2$ (H and H'), $Bx > brZ4$ (I and I'), $Bx > br^{RNAi}$ (J and J'), and $Bx > EcR.A^{DN}$ (K and K'). Yellow arrows indicate primary area of expression. (Scale bar, 50 μ m.) (L–M) Representative images of Wg (gray) expression in control, UAS-GFP alone (L), and UAS- $EcR.A^{DN}$;UAS-GFP (M), MARCM clones. Larvae were heat-shocked at 60 h AED, and tissues were isolated at 104 h AED. Zoom-in images of clones at the hinge (L' and L'') and margin (M' and M'') are shown on the right. Arrows indicate the region where clones cross the Wg expression at the hinge (yellow) and margin (blue). Scale bar, 50 μ m.) (N) Wg locus transcriptional activity - UAS- $EcR.A^{DN}$;UAS-GFP clones in wg-lacZ background. N' and N'' show clones at hinge and margin, respectively. (O) Ecdysone signaling cascade for the regulation of Wg expression.

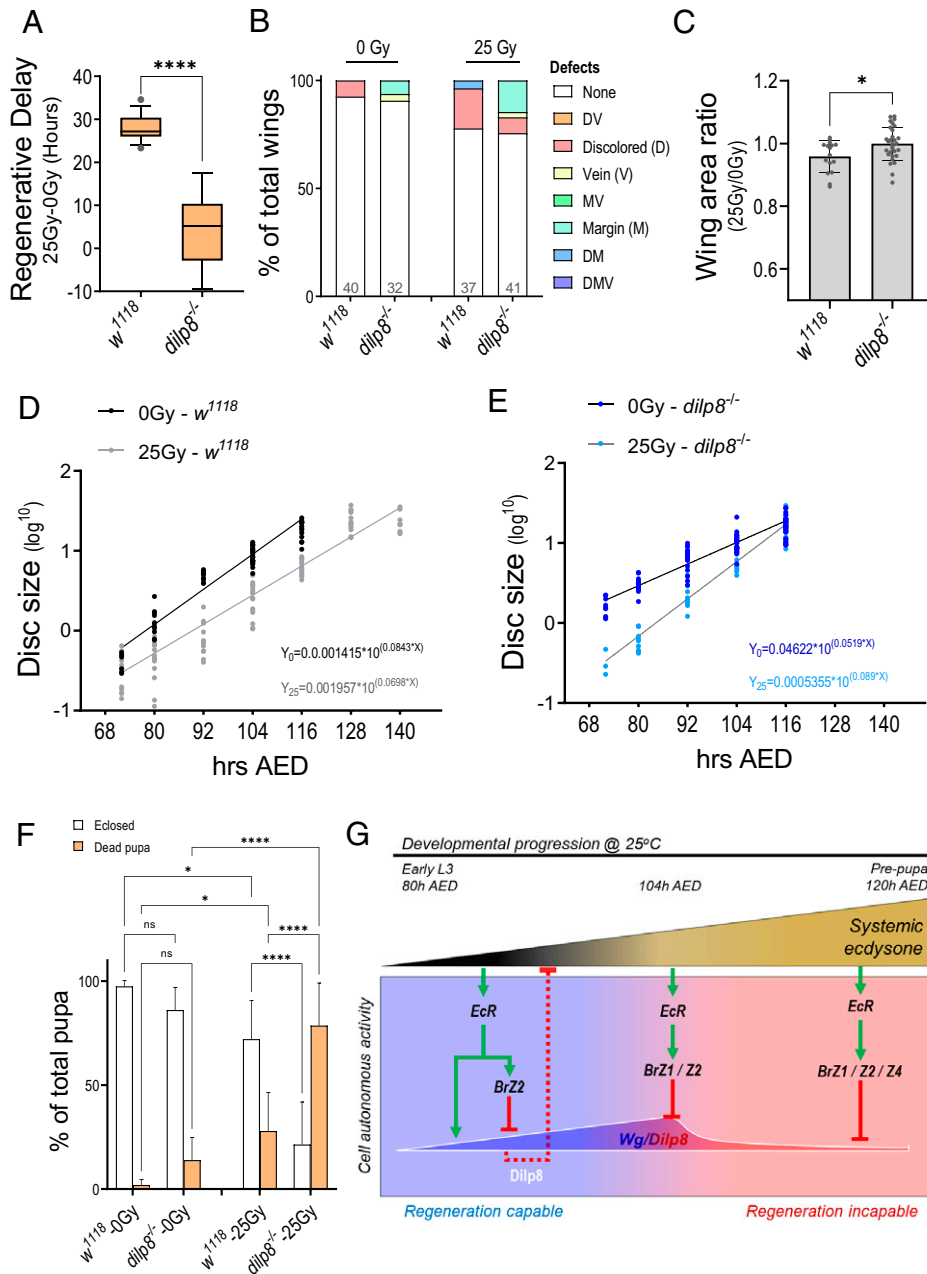


Fig. 6. *Dilp8*⁻ larvae meet regeneration targets within the attenuated development period. (A) Quantification of regenerative delay following early damage (20 Gy, 80 h) in *w*¹¹¹⁸ (*dilp8*⁺) and *dilp8*^{-/-} larvae. Unpaired *t* test, *****P* < 0.0001. (B and C) *dilp8*^{-/-} adult wings show no increase in defects (B) or size mismatch (C) following early damage. (B) The percentage of defective adult wings following no damage (0 Gy) and early damage (25 Gy, 80 h) in *w*¹¹¹⁸ and *dilp8*^{-/-} adults. Population size is indicated in graph. (C) Quantification of adult wing size, measured in unit area and normalized to size of undamaged wings in respective genotype and sex. Unpaired *t* test, **P* < 0.05. (D and E) Exponential growth analysis of wing discs following no damaged tissues (0 Gy) and damage (25 Gy) at 48 h AED in *w*¹¹¹⁸ (D) and *dilp8*^{-/-} (E) larvae. Datasets normalized to 72 h undamaged *w*¹¹¹⁸ tissues. *R*² values in *SI Appendix*, Fig. S11. (F) Quantification of population viability following early damage (20 Gy, 80 h) in *w*¹¹¹⁸ and *dilp8*^{-/-} larvae. *****P* < 0.0001, **P* < 0.05, two-way ANOVA with Tukey's test. (G) The summary model illustrates the sequence of ecdysone-regulated cell-autonomous events that regulate regenerative activity and regenerative capacity during wing disk development.

(pupal cases where the adults fail to eclose) in control larvae is relatively low, typically ~25% for larvae irradiated at 25 Gy. However, pupal lethality of irradiated *dilp8*⁻ larvae is much higher, ~78% (Fig. 6F). We believe that the increase in pupal lethality is a consequence of regenerative activity in *dilp8*⁻ larvae as control larvae irradiated late (post-RRP), which fail to initiate a regenerative response, still produce a relatively low rate of pupal lethality (~30%) (*SI Appendix*, Fig. S11D). Therefore, Dilp8 checkpoint activation appears to play an essential

role in preserving the future pupal viability of animals undergoing disk regeneration.

Discussion

Regenerating imaginal discs release Dilp8, which circulates in the hemolymph and signals through Lgr3 in the brain and PG to limit ecdysone production (8, 9, 11–13). By delaying the ecdysone increase that signals the end of larval development,

Dilp8 extends the larval development period for regeneration (8, 9). However, we demonstrate here that even in the absence of Dilp8 signaling, damaged wing imaginal discs are capable of the repatterning and regrowth required to reach their regeneration target in an attenuated regenerative period (Fig. 6B and C). However, we see that the accelerated regeneration in *dilp8*⁻ larvae is also accompanied by a substantial increase in pupal lethality (Fig. 6F). This pupal lethality does not appear to result from unrepaired damage, as larvae irradiated post-RRP when a regenerative response cannot be initiated do not show increased pupal lethality (*SI Appendix*, Fig. S11D). Therefore, the role of Dilp8 and regenerative checkpoint may be primarily to preserve viability in the presence of regenerating tissues as opposed to providing adequate time for regeneration. In this study, we did not examine how regeneration checkpoint activation preserves pupal viability. Still, one possibility is that an extended larval feeding period allows larvae with regenerating tissues the ability to store up sufficient energy reserves for both regeneration and completion of metamorphosis. Further study is necessary to determine how regeneration impacts pupal viability.

In contrast to *dilp8*⁻ larvae, which can produce completely regenerated tissues in an attenuated regenerative period, artificially increasing ecdysone levels through feeding increases the number of incompletely regenerated tissues substantially (*SI Appendix*, Fig. S2C and D). This suggests that the changing ecdysone levels that occur throughout the regenerative period of larval development exert sensitive control over imaginal disk regeneration and that this regulation is lost when we ectopically manipulate ecdysone levels. In this study, we demonstrate that ecdysone plays a dual role in regulating regenerative activity in damaged discs to ensure that regeneration targets are achieved within the larval period. (summarized in Fig. 6G). First, we demonstrate that ecdysone signaling in damaged imaginal discs is necessary for the up-regulation of Wg and Dilp8, critical signals mediating the local and systemic regenerative responses (Fig. 1L–N). This observation may reflect a requirement for ecdysone signaling in Wg expression at the hinge region (Fig. 5L–N), which is critical to irradiation-induced regenerative responses (22). As development progresses through the L3, ecdysone pulses from the PG cause ecdysone to accumulate in the larvae (15). We propose that this accumulation initiates a series of concentration-dependent events (Fig. 2B–F). First, ecdysone promotes regeneration, accelerating regenerative activity as ecdysone titer increases. Then, when ecdysone titer reaches a high level in the larvae, ecdysone signaling suppresses regenerative activity by activating the expression of the Broad splice isoforms (Fig. 3), which suppress regenerative activity in damaged discs (Fig. 4).

This biphasic, concentration-dependent regulation of regenerative activity allows ecdysone to coordinate regeneration with the duration of larval development. This coordinating role may be similar to how ecdysone coordinates imaginal disk patterning with the larval development period (38). Similarly, recently published experiments have observed that damage of the *Drosophila* hindgut during L2 or early L3 produces Dilp8, delaying the onset of pupariation, whereas damage to the hindgut of wandering L3 larvae no longer produces Dilp8 or developmental delay. However, regeneration is still completed in this attenuated period through accelerated mitotic cycling, which allows the tissue to meet the regeneration target within the mitotic regeneration window (39). In this example, while ecdysone signaling regulates the end of mitotic regeneration, the role of ecdysone signaling in producing accelerated mitoses has not been investigated.

Other pathways have been implicated in regulating regenerative activity in the wing disk or the loss of regenerative capacity at the end of development. Further experiments will be

required to determine how these pathways are regulated by ecdysone and Broad. Recent work by Narbonne-Reveau and Maurange (20) has demonstrated that Chinmo, which regulates the “stemness” of cells, is expressed during early wing disk development and antagonizes the expression of the BrZ1 splice isoform to allow regenerative activity. Reciprocally, BrZ1 also antagonizes the expression of Chinmo. In contrast to this work, which only identified BrZ1 expression in wing discs, we demonstrate here that three Broad isoforms (BrZ1, Z2, and Z4) are expressed in the wing disk and can act to limit regenerative capacity, with BrZ4 producing the strongest phenotypic effect. We also demonstrate that these isoforms are expressed during regeneration and potentially function to limit the duration of regenerative activity. It is unclear how BrZ2, which is expressed earliest in third-instar wing development, shares the same antagonistic interaction with Chinmo as BrZ1. Nor is it clear whether the lower ecdysone levels prior to the RRP act to promote, instead of antagonize, Chinmo expression. In addition, since Chinmo promotes EcR expression in other tissues (40), it is possible that Chinmo may also promote regenerative activity by enhancing ecdysone signaling. Subsequent experiments will be necessary to address these questions.

At the end of larval development, the *Drosophila* genome undergoes extensive epigenetic changes in preparation for pupation and metamorphosis (41, 42). The Polycomb-group proteins (PcG) produce silencing modifications on the heterochromatin at *wgDRE* to block regeneration after the RRP (34). However, it remains unclear how PcG is recruited to the *wgDRE*. There is a putative Pc-binding site in the *wgDRE*, but it is not necessary for silencing this locus at the end of larval development (34). Both PcG and Broad are essential for suppressing regeneration genes, and there is evidence that Broad and PcG physically interact during the wing disk development (43). Therefore, it is possible that Broad isoforms may recruit PcG to *wgDRE* to suppress regeneration at the end of larval development.

In summary, our findings provide insight into the mechanisms that coordinate tissue regeneration with the development of the animal as a whole. The steroid hormone ecdysone has a biphasic, concentration-dependent effect on the regenerative activity of the *Drosophila* wing imaginal disk. Through biphasic signaling, ecdysone can coordinate the completion of regeneration with the end of the larval period of growth in wild-type larvae and larvae that lack the regeneration checkpoint, where the regenerative period is attenuated. We demonstrate that the regeneration checkpoint may be important for maintaining pupal viability in animals that have regenerated their imaginal discs.

Materials and Methods

***Drosophila* Culture.** Experimental lines and crosses were maintained at 25°C with 12-h alternating light/dark cycles. The developmental timing was synchronized by staging egg-laying on grape agar plates (Genesee Scientific) during a designated 4-h interval. After embryo hatching, 24 h AED, 20 first-instar larvae were transferred into vials or plates containing standard (cornmeal-yeast-molasses) media (Archon Scientific B101). The larvae remained undisturbed in the media at 25°C or 18°C until treatments began in third larval instar.

Irradiation Damage and Ecdysone Feeding. Staged larvae were left undamaged or exposed to 20 or 25 Gy X-irradiation generated from a 43805N X-ray system Faxitron operating at 130 kV and 3.0 mA. The larvae were exposed to x-irradiation at 80 h AED, 92 h AED (*SI Appendix*, Figs. S1 and S10), or 104 h AED.

Ecdysone food was prepared by dissolving 20-hydroxyecdysone (Sigma #H5142; starting concentration: 20 mg/mL in 95% ethanol) in 2 mL of standard food media at final concentrations of 0.1, 0.3, 0.6, and 1.0 mg/mL, or an equivalent volume of 95% ethanol (0 mg/mL) for control. Whereas as little as 20 nM ecdysone can support disk growth in vitro, since ecdysone is being introduced by supplementing larval food, it produces much smaller changes in circulating

hemolymph ecdysone concentration. Larvae were reared as previously described until 80 h AED, then transferred to the ecdysone or ethanol-control food, approximately six to seven larvae per vial (5).

Western Blot. Proteins were extracted in 50 μ L SDS lysis buffer (2% SDS, 60 mM Tris-Cl pH6.8, 1 \times protease inhibitors, 5 mM NaF, 1 mM Na orthovanadate, 1 mM β glycerolphosphate in dH₂O), sonicated using two 5-s pulses (microtip Branson sonifier), boiled for 10 min at 95 °C, and centrifuged at 15,000 rpm for 5 min at room temperature. The supernatant was collected for BCA assay and analyzed by SDS/PAGE using Mini-Protean TGXTM 4–15% (Bio-Rad) and transferred to nitrocellulose membranes. For Western blot analysis, membranes were incubated with blocking solution (1% cold water fish gelatin; Sigma #G7765), primary antibodies (1:500 Broad Core, DSHB #25E9.D7 and 1:10,000 α -tubulin, Sigma #T6074), followed by appropriate LI-COR IRDye

secondary antibodies and visualized using the LI-COR Odyssey CLx Imaging System. Quantifications were done using LI-COR Image Studio Software.

Data Availability. All study data are included in the article and *SI Appendix*. *Drosophila* stocks that were generated to complete these studies are available upon request.

ACKNOWLEDGMENTS. We thank Iswar Hariharan and Rob Harris for the *wgDRE* reporter lines; Andre Landin Malt, Brittany Martinez, and Danielle DaCrema for Western blot reagents and assistance; and the University of Virginia Advanced Microscopy Facility (RRID: SCR_018736) for training and access to the Zeiss LSM700 and LSM710 confocal microscopes used in this study. This work was supported by NIH Grant R01 GM099803 (to A.H.) and GM008715 (to F.K.), and by March of Dimes Basil O'Connor Award 5FY1260 (to A.H.).

1. M. H. Yun, Changes in regenerative capacity through lifespan. *Int. J. Mol. Sci.* **16**, 25392–25432 (2015).
2. A. W. Seifert, S. R. Voss, Revisiting the relationship between regenerative ability and aging. *BMC Biol.* **11**, 2 (2013).
3. L. N. Marshall *et al.*, Stage-dependent cardiac regeneration in *Xenopus* is regulated by thyroid hormone availability. *Proc. Natl. Acad. Sci. U.S.A.* **116**, 3614–3623 (2019).
4. K. Hirose *et al.*, Evidence for hormonal control of heart regenerative capacity during endothermy acquisition. *Science* **364**, 184–188 (2019).
5. A. Halme, M. Cheng, I. K. Hariharan, Retinoids regulate a developmental checkpoint for tissue regeneration in *Drosophila*. *Curr. Biol.* **20**, 458–463 (2010).
6. N. Yamanaka, K. F. Rewitz, M. B. O'Connor, Ecdysone control of developmental transitions: Lessons from *Drosophila* research. *Annu. Rev. Entomol.* **58**, 497–516 (2013).
7. R. B. Hodgetts, B. Sage, J. D. O'Connor, Ecdysone titers during postembryonic development of *Drosophila melanogaster*. *Dev. Biol.* **60**, 310–317 (1977).
8. J. Colombani, D. S. Andersen, P. Léopold, Secreted peptide Dilp8 coordinates *Drosophila* tissue growth with developmental timing. *Science* **336**, 582–585 (2012).
9. A. Garelli, A. M. Gontijo, V. Miguela, E. Caparros, M. Dominguez, Imaginal discs secrete Insulin-like peptide 8 to mediate plasticity of growth and maturation. *Science* **336**, 579–582 (2012).
10. A. Garelli *et al.*, Dilp8 requires the neuronal relaxin receptor Lgr3 to couple growth to developmental timing. *Nat. Commun.* **6**, 8732 (2015).
11. J. S. Jaszczak, J. B. Wolpe, R. Bhandari, R. G. Jaszczak, A. Halme, Growth coordination during *Drosophila melanogaster* imaginal disc regeneration is mediated by signaling through the relaxin receptor Lgr3 in the prothoracic gland. *Genetics* **204**, 703–709 (2016).
12. D. M. Vallejo, S. Juarez-Carreno, J. Bolivar, J. Morante, M. Dominguez, A brain circuit that synchronizes growth and maturation revealed through Dilp8 binding to Lgr3. *Science* **350**, aac6767 (2015).
13. J. Colombani *et al.*, *Drosophila* Lgr3 couples organ growth with maturation and ensures developmental stability. *Curr. Biol.* **25**, 2723–2729 (2015).
14. J. F. Hackney, O. Zolali-Meybodi, P. Cherbas, Tissue damage disrupts developmental progression and ecdysteroid biosynthesis in *Drosophila*. *PLoS One* **7**, e49105 (2012).
15. O. Lavrynenko *et al.*, The ecdysteroidome of *Drosophila*: Influence of diet and development. *Development* **142**, 3758–3768 (2015).
16. K. Madhavan, H. A. Schneiderman, Hormonal control of imaginal disc regeneration in *Galleria Mellonella* (Lepidoptera). *Biol. Bull.* **137**, 321–331 (1969).
17. T. Kunieda, S. Kurata, S. Natori, Regeneration of *Sarcophaga* imaginal discs in vitro: Implication of 20-hydroxyecdysone. *Dev. Biol.* **183**, 86–94 (1997).
18. P. M. Hopkins, Ecdysteroids and regeneration in the fiddler crab *Uca pugilator*. *J. Exp. Zool.* **252**, 293–299 (1989).
19. S. Das, D. S. Durica, Ecdysteroid receptor signaling disruption obstructs blastemal cell proliferation during limb regeneration in the fiddler crab, *Uca pugilator*. *Mol. Cell. Endocrinol.* **365**, 249–259 (2013).
20. K. Narbonne-Reveau, C. Maurange, Developmental regulation of regenerative potential in *Drosophila* by ecdysone through a bistable loop of ZBTB transcription factors. *PLoS Biol.* **17**, e3000149 (2019).
21. R. K. Smith-Bolton, M. I. Worley, H. Kanda, I. K. Hariharan, Regenerative growth in *Drosophila* imaginal discs is regulated by Wingless and Myc. *Dev. Cell* **16**, 797–809 (2009).
22. S. Verghese, T. T. Su, *Drosophila* Wnt and STAT define apoptosis-resistant epithelial cells for tissue regeneration after irradiation. *PLoS Biol.* **14**, e1002536 (2016).
23. K. F. Rewitz, N. Yamanaka, M. B. O'Connor, Developmental checkpoints and feedback circuits time insect maturation. *Curr. Top. Dev. Biol.* **103**, 1–33 (2013).
24. L. Cherbas, X. Hu, I. Zhimulev, E. Belyaeva, P. Cherbas, EcR isoforms in *Drosophila*: Testing tissue-specific requirements by targeted blockade and rescue. *Development* **130**, 271–284 (2003).
25. C. A. Bayer, B. Holley, J. W. Fristrom, A switch in broad-complex zinc-finger isoform expression is regulated posttranscriptionally during the metamorphosis of *Drosophila* imaginal discs. *Dev. Biol.* **177**, 1–14 (1996).
26. P. R. DiBello, D. A. Withers, C. A. Bayer, J. W. Fristrom, G. M. Guild, The *Drosophila* Broad-complex encodes a family of related proteins containing zinc fingers. *Genetics* **129**, 385–397 (1991).
27. I. Kiss, A. H. Beaton, J. Tardiff, D. Fristrom, J. W. Fristrom, Interactions and developmental effects of mutations in the Broad-complex of *Drosophila melanogaster*. *Genetics* **118**, 247–259 (1988).
28. L. von Kalm, K. Crossgrove, D. Von Seggern, G. M. Guild, S. K. Beckendorf, The Broad-complex directly controls a tissue-specific response to the steroid hormone ecdysone at the onset of *Drosophila* metamorphosis. *EMBO J.* **13**, 3505–3516 (1994).
29. I. F. Emery, V. Bedian, G. M. Guild, Differential expression of Broad-complex transcription factors may forecast tissue-specific developmental fates during *Drosophila* metamorphosis. *Development* **120**, 3275–3287 (1994).
30. D. Jia, J. Bryant, A. Jevitt, G. Calvin, W. M. Deng, The ecdysone and Notch pathways synergistically regulate Cut at the dorsal-ventral boundary in *Drosophila* wing discs. *J. Genet. Genomics* **43**, 179–186 (2016).
31. P. P. D'Avino, S. Crispi, L. C. Polito, M. Furia, The role of the BR-C locus on the expression of genes located at the ecdysone-regulated 3C puff of *Drosophila melanogaster*. *Mech. Dev.* **49**, 161–171 (1995).
32. M. Schubiger, A. Sustar, G. Schubiger, Regeneration and transdetermination: The role of *wingless* and its regulation. *Dev. Biol.* **347**, 315–324 (2010).
33. R. E. Harris, M. J. Stinchfield, S. L. Nystrom, D. J. McKay, I. K. Hariharan, Damage-responsive, maturity-silenced enhancers regulate multiple genes that direct regeneration in *Drosophila*. *eLife* **9**, e58305 (2020).
34. R. E. Harris, L. Setiawan, J. Saul, I. K. Hariharan, Localized epigenetic silencing of a damage-activated WNT enhancer limits regeneration in mature *Drosophila* imaginal discs. *eLife* **5**, e11588 (2016).
35. J. S. Jaszczak, J. B. Wolpe, A. Q. Dao, A. Halme, Nitric oxide synthase regulates growth coordination during *Drosophila melanogaster* imaginal disc regeneration. *Genetics* **200**, 1219–1228 (2015).
36. J. S. Jaszczak, A. Halme, Arrested development: Coordinating regeneration with development and growth in *Drosophila melanogaster*. *Curr. Opin. Genet. Dev.* **40**, 87–94 (2016).
37. D. S. Andersen, J. Colombani, P. Léopold, Coordination of organ growth: Principles and outstanding questions from the world of insects. *Trends Cell Biol.* **23**, 336–344 (2013).
38. A. N. Alves, M. M. Oliveira, T. Koyama, A. Shingleton, C. Mirth, Ecdysone coordinates plastic growth with robust pattern in the developing wing. *bioRxiv* [Preprint] (2020). <https://www.biorxiv.org/content/10.1101/2020.12.16.423141v3>. Accessed 1 August 2021.
39. E. Cohen, N. G. Peterson, J. K. Sawyer, D. T. Fox, Accelerated cell cycles enable organ regeneration under developmental time constraints in the *Drosophila* hindgut. *Dev. Cell* **56**, 2059–2072.e3 (2021).
40. G. Marchetti, G. Tavosanis, Steroid hormone ecdysone signaling specifies mushroom body neuron sequential fate via Chinmo. *Curr. Biol.* **27**, 3017–3024.e4 (2017).
41. P. Saha, D. T. Sowpati, R. K. Mishra, Epigenomic and genomic landscape of *Drosophila melanogaster* heterochromatic genes. *Genomics* **111**, 177–185 (2019).
42. Y. Ma, L. Buttitta, Chromatin organization changes during the establishment and maintenance of the postmitotic state. *Epigenetics Chromatin* **10**, 53 (2017).
43. X. Lv *et al.*, A positive role for polycomb in transcriptional regulation via H4K20me1. *Cell Res.* **26**, 529–542 (2016).